RASĀYAN *J. Chem.*
Vol. 17 | No. 1 |154-164| January - March | 2024
ISSN: 0974-1496 | e-ISSN: 0976-0083 | CODEN: RJCABP
http://www.rasayanjournal.com
http://www.rasayanjournal.co.in

GRAPHENE OXIDE DERIVED FROM CASSAVA PEEL AS A POTENTIAL ADSORBENT FOR TETRACYCLINE REMOVAL FROM AQUEOUS ENVIRONMENT

Rinawati✉, P. Pirdaus, A. Rahmawati, Buhani and A.A. Kiswandono
Department of Chemistry, Faculty of Mathematics and Natural Sciences,
University of Lampung, Indonesia
✉Corresponding Author: rinawati@fmipa.unila.ac.id

ABSTRACT

Due to the increase in bacterial resistance, the presence of antibiotic residues in ambient water is becoming a serious problem. In order to stop antibiotic-related water contamination, graphene oxide has been extensively employed as an advanced adsorbent. In this study, cassava peel was utilized to create graphene oxide, which was then applied as an adsorbent to remove tetracycline. The modified Hummers technique was used to produce graphene oxide, along with an oxidizing agent. Studies have been done on graphene oxide characterization and adsorption process optimization. According to the study, tetracycline removal was best accomplished under settings that included an adsorbent mass of 20 mg, an antibiotic concentration of 10 ppm, a pH of 5, and a contact period of 10 minutes. The adsorbent substance has shown promise in removing tetracycline from aqueous environments.

Keywords: Adsorbent; Agriculture Waste; Graphene Oxide; Tetracycline.

RASĀYAN *J. Chem.*, Vol. 17, No.1, 2024

INTRODUCTION

The use of antibiotics in human medicine for the treatment and prevention of illnesses, as well as in agricultural sectors for the development and production of animals and plants, has been widespread across the world.[1] Antibiotic usage has reportedly increased significantly during the COVID-19 outbreak. Antibiotic residues are a result of this, and they have recently become a significant problem, particularly in aquatic environments.[2] Tetracycline is a common antibiotic used in human health, agriculture, and the animal sector because of its high quality and reasonable price.[3] Tetracycline antibiotics are either directly or indirectly released into the aquatic environment, which can result in pollution. Antibiotics used by people and animals are around 30%–90% excreted through feces and urine as unaltered parent chemicals.[4,5] Due to the release of antibiotic residues from wastewater treatment facilities, veterinary waste, and agricultural runoff, they are frequently discovered in soil, surface water, groundwater, milk, and drinking water.[6] The widespread use of antibiotics can have several negative consequences, including acute and long-term toxicity, damage to aquatic photosynthetic organisms, disruption of the native microbial community, and the proliferation of antibiotic-resistant genes in microorganisms.[7-10] Tetracycline antibiotics, in particular, have been found to impair crucial soil activities, such as microbial soil respiration,[11] reduction of Fe(III),[12] nitrogenization activities,[13,14] and phosphatase.[15] To remove this contamination from aquatic habitats, it is necessary to address this issue and take action to reduce the overuse of antibiotics.[16-18] Antibiotics can be eliminated using a variety of methods, including membrane removal,[19,20] degradation,[21–23] electrochemical approaches,[24,25] and adsorption.[26] Adsorption is one alternative strategy that has the benefits of being inexpensive, simple to build, and simple to use.[27] Activated carbon,[28] chitosan particles,[29] coal humic acid,[30] and smectite clay[31] have all been found to have the potential to adsorb and remove tetracycline antibiotics. However, there is an increasing need to create techniques that are both effective and affordable to get rid of these pollutants.[32,33] The huge surface area and superior adsorption capability of the carbon nanostructured materials, including graphene oxide, make them suited for application as adsorbents.[34-36] Graphene oxide has oxygen functional groups such as carboxyl, carbonyl, epoxy, and hydroxyl groups that increase its activity.[37] According to reports, graphene oxide may remove heavy metals,[38] organic pollutants,[39] antibiotics.[40] Graphene oxide has historically been derived from non-renewable minerals, however, to support sustainability and facilitate the accessibility of graphene oxide, various efforts have

http://doi.org/10.31788/RJC.2024.1718640

been made to produce graphene oxide or graphene oxide using alternative sources that are abundant, cost-effective, and environmentally friendly.[41] Using inexpensive adsorbents made from agricultural waste has been recognized as an environmentally responsible adsorption strategy. These adsorbents assist in reducing agricultural waste and fostering its recovery and reuse in addition to aiding in the removal of contaminants like antibiotics from aquatic environments. Agricultural waste, including maize cobs, rice grains, soybean dregs, and cassava peels, can be a substitute supply of adsorbent material in agricultural nations like Indonesia. According to data from the Bureau of Central Statistics,[42] Lampung Province is Indonesia's top cassava grower, with an annual production of 6.683 million tons and an average yield of 25 tons per hectare. Following this rise in cassava output comes a rise in cassava peel trash that hasn't been properly used. This waste has the potential to be employed as a raw material for the synthesis of graphene oxide due to its high cellulose content and somewhat high carbon content.[31] The objective of this study was to investigate the potential use of graphene oxide derived from cassava peel as an adsorbent for the removal of tetracycline from aqueous solutions. To validate the graphene oxide, the produced material was examined by X-Ray Diffraction (XRD), Fourier Transform Infrared (FTIR), Raman, UV-Vis, and Scanning Electron Microscopy-Energy Dispersive X-ray (SEM-EDX). To achieve maximum adsorption, optimization of various parameters is essential. This study assesses the influence of different adsorbent masses, pH levels, starting adsorbate concentrations, contact times, and desorption solvents. The examination involves making adjustments to these parameters to comprehend their effects on the adsorption process.

EXPERIMENTAL

Material and Methods

Cassava peel waste was employed as one of the chemicals in this experiment. Standard tetracycline hydrochloride was acquired from Sigma-Aldrich, and other chemicals were of the analytical reagent grade and weren't further purified before usage. Glassware, a magnetic stirrer hot plate, a centrifuge, an oven, an ultrasonic pH meter, an X-ray diffractometer (PANalytical X'Pert3 Powder), an energy dispersive X-ray scanning electron microscope (EVO® MA 10), and an ultraviolet-visible spectrophotometer (Agilent Cary 100) were used in this experiment.

General Procedure

Synthesis of Graphite from Cassava Peel

Cassava peel waste was divided into small pieces, rinsed many times in water to remove dirt and dust, and then dried for two to three days in the sun and for one and a half hours in a hot oven. The dried cassava peel was crushed into a powder, which was then added to a crucible cup in an amount of up to 6 g and heated for 2 hours at 350 °C. To be employed in the following step, the acquired charcoal is crushed using a mortar after cooling in a desiccator for 15 minutes.[43] 5 g of carbonized charcoal was weighed out and placed into a 1000 mL beaker glass. 500 mL of distilled water was added, and the mixture was stirred at 600 rpm with a magnetic stirrer. Next, 4 mL of the $FeCl_3.6H_2O$ solution was added, and the rotation speed was raised to 900 rpm at room temperature. By gradually adding 1 M HCl, the pH of the combined solution was brought near to pH 2, and it was then agitated at 60 °C for 5 hours. To separate the supernatant from the graphite precipitate, the solution was centrifuged. After being rinsed in distilled water, the precipitate's pH was raised to 7, at which point it was dried in an oven at 50 °C for 8 hours and then at 110 °C for 5 hours. After cooling in the oven, samples are placed in a desiccator for 15 minutes.[43]

Synthesis of Graphene Oxide with Modified Hummers

In a fume hood, 1 g of graphite was placed into a beaker. Next, 23 mL of concentrated H_2SO_4 was added, and the mixture was agitated for 30 min in an ice bath (0 °C) using a magnetic stirrer. 3 g of $KMnO_4$ were gradually added to the mixed solution while the temperature was kept below 10 °C. The temperature was raised to 98 °C while 46 mL of distilled water was gradually added after 30 minutes of stirring at 35 °C. The mixture was then allowed to stand for 15 minutes.[34] 10 minutes of stirring and the addition of 140 mL of distilled water were followed by the addition of 10 mL of a 30% H_2O_2 solution to stop the reaction. 5% HCl solution was used to rinse the resultant suspension many times until the sulfate disappeared, tested with barium chloride, and periodically cleaned with distilled water until the pH reached 5. After that, the precipitate and solution were separated using centrifugation for 10 minutes at 5000 rpm. To create graphene

oxide, after being combined with 450 mL of distilled water, the precipitate was sonicated for 2 hours. After that, the filtrate was dried for 5 hours at 60 °C in an oven.[44]

Detection Method

Characterization of Graphene Oxide

With the use of FT-IR and Raman spectroscopy, the properties of the functional groups in graphene oxide were determined. Graphene oxide surface morphology and quantitative content were studied using SEM-EDX. XRD was used to determine the molecule's crystalline phase.

Optimization of Tetracycline Antibiotic Adsorption

A beaker glass was filled with graphene oxide at various concentrations of 5; 10; 15; 20 and 25 mg/g, and 10 mL of a standard tetracycline solution at 10 ppm was added. After stirring the resultant mixture for 30 minutes, graphene oxide was extracted from the solution by centrifuging it for 15 minutes at 10,000 rpm. The filter paper was used to filter the solution, and a UV-Vis spectrophotometer operating at a wavelength of 356 nm was used to evaluate the filtrate. The other optimization involved changing the pH, the amount of adsorbate, the contacting period, and the desorption solution.

RESULTS AND DISCUSSION

Synthesis of Graphene Oxide

Different colors that appeared during the production process were proof that graphene oxide had formed. A thick green solution quickly appeared after adding an acid combination to a beaker containing a mixture of graphite and potassium permanganate, suggesting the synthesis of dimanganese heptoxide (Mn_2O_7) and an increase in temperature from room temperature to 50 °C. Exothermic redox processes were present, as evidenced by the temperature increase that was seen. The initially created thick slurry solution then progressively changed into a brown solution as a result of constant stirring and heating, adding support to the previously reported effective synthesis of graphene oxide.[45]

Characterization of Graphene Oxide by FT-IR

Figure-1 displays the outcome of FT-IR characterization. The stretching vibrations of the O−H bond (hydroxyl group) is seen as a prominent band at 3204 cm^{-1} in the IR spectra of materials that resemble graphene oxide. Because graphene oxide is hydrophilic and allows water molecules to adsorb on its surface, this band is present.[44] Additionally, there is absorption at 1706 cm^{-1}, which shows that C=O (carbonyl) groups are being absorbed. Additionally measured absorptions at 1359 cm^{-1} and 1034 cm^{-1} show that the produced graphene oxide contains C−O−C (epoxy) groups. The functional groups in modified graphene oxide Hummers have oxygen groups, namely carbonyl (−C=O), carboxyl (−COOH), and hydroxyl (−OH), as was discussed above. The presence of a functional group that is appropriate for pure graphene oxide in this FT-IR spectrum demonstrates that the production of graphene oxide was effective.[37]

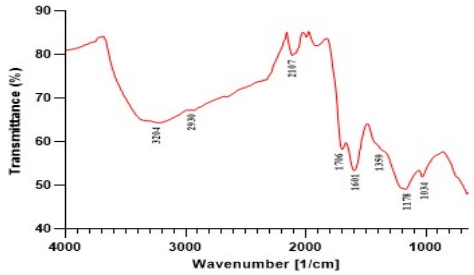

Fig.-1: FTIR Spectrum of Graphene Oxide Derived from Cassava Peel

Characterization using X-ray Diffraction (XRD)

The graphene oxide's XRD pattern in Fig.-2 shows an amorphous diffractogram with one dominating peak at 24.71° in the 2 area, which is typical for these carbons.[46] The use of raw materials derived from natural resources can be attributed to the sample's existence of the amorphous phase.[47]

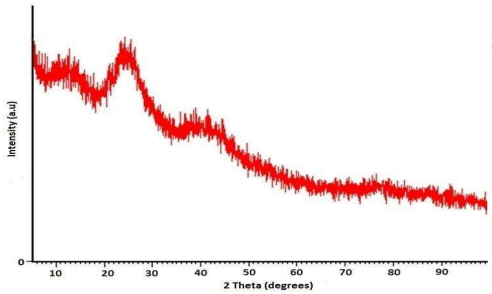

Fig.-1: XRD Diffractogram of Modified Graphene Oxide Hummers

Given that graphene oxide is a natural compound that is difficult to crystallize, it is known from Fig.-2 that the diffractogram pattern for this material likewise manifests at the peak of the 2θ area of 10° with an amorphous diffractogram pattern. Another study[48] also came to the same conclusions, finding that the amorphous peak shapes in the MGOS XRD spectra before and after adsorption on tetracycline were almost identical. The graphene oxide peak's diminished intensity at an angle of 2θ 10.1° and its shift to 7.9° are the primary distinctions. Strength declines, which suggests a decline in crystal level. Tetracycline adsorption results in an increase in the layer gap between graphene oxide sheets, which may be the result of tetracycline molecules intercalating into the intercalation of the graphene oxide sheets, as shown by the 2θ angle shift in the smaller direction.

Characterization using Scanning Electron Microscopy (SEM)

The graphene oxide surface morphology, which appears as a sheet-like structure in Fig.-3 SEM picture, is typical of graphene oxide. Exfoliation of the graphene oxide surface is shown to generate distinct thin layers with a smooth surface and wrinkled region. This picture also demonstrates that samples, as described in the previous research, have strata with various degrees of transparency.[49] The graphene oxide surface also has several protrusions and curved forms.

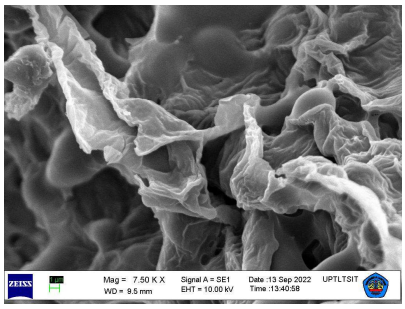

Fig.-2: SEM Image of Graphene Oxide Derived from Cassava Peel

Characterization using Raman Spectra

Figure-4 displays the graphene oxide's Raman spectrum. Two peaks, representing the D band and the G band, can be seen in the picture at wave numbers 1363 cm^{-1} and 1598 cm^{-1}, respectively. The D band is produced by vibrational modes linked to edges, accompanying impurities, and structural flaws in graphite. The sp^3 carbons in graphene sheets have been stretched, as shown by the distinctive D-bands.

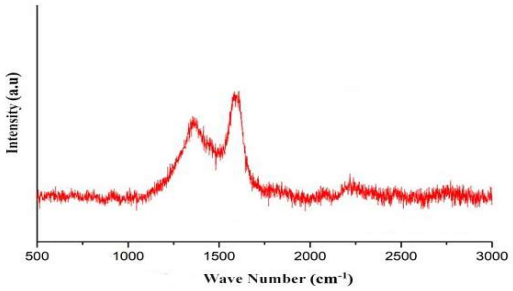

Fig.-3: The Raman Spectra of Graphene Oxide Derived from Cassava Peels

The G-bands, which result from vibrations in the typical graphite structure, are visible in the illustration. It is equivalent to stretching sp^2 carbon. These two peaks, which are characteristic Raman vibrational modes for carbon-based materials, show that the reported graphene oxide contains sp^2-hybridized carbon. Our Raman results are consistent with Sujiono *et al.*[47] method of characterizing graphene oxide made from discarded coconut shells, and with Somanathan *et al.*[50] utilization of graphene oxide made from sugarcane bagasse.

Adsorption of Tetracycline with Graphene Oxide

Figure-5 shows the tetracycline adsorption spectrum onto graphene oxide. At 275 and 356 nm, the tetracycline spectrum shows absorption peaks. These absorption peaks, however, are no longer visible in the tetracycline spectrum after adsorption with graphene oxide. This shows that the tetracycline and graphene oxide surface had an adsorption relationship. Tetracycline and the graphene oxide surface are said to have formed hydrogen bonds and interacted with each other to cause this adsorption. These results are in line with what Ai *et al.*[51] stated.

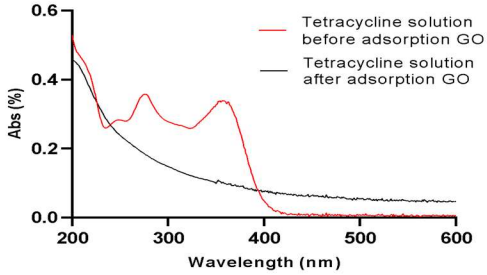

Fig.-4: UV-Vis Spectrum of Adsorption Tetracycline Solution with Graphene Oxide

Adsorption kinetics and Adsorption Isotherm

The Langmuir and Freundlich equations were used to fit the observed adsorption isotherms, and the adsorption kinetics were modeled using the pseudo-first- and pseudo-second-order. According to research findings, tetracycline was absorbed by free graphene oxide dispersion within 90 minutes. Tetracycline may easily diffuse onto the graphene oxide surface as all of its surfaces are accessible to the solvent.[48] In contrast, it takes more time for diffusion to reach the inner surface of graphene oxide. On graphene composites, other studies also noted slower antibiotic kinetics. For instance, Yu *et al.*[52] discovered that it took 24 hours for ciprofloxacin adsorption on sodium alginate or graphene oxide beads to plateau. Ciprofloxacin adsorption on composites made of graphene and soy protein took 24 hours to reach equilibrium, according to Zhuang *et al.*[53] Tetracycline adsorption on GO-Fe_3O_4 did, however, approach a plateau after 10 minutes, as demonstrated by Lin *et al.*[54]. Fast kinetics and a relatively low capacity for adsorption show that the majority of adsorption only happens on the outer surface of GO-Fe_3O_4. Pseudo-first-order and pseudo-second-order models were used to assess the kinetic data. Compared to the pseudo-first-order model, which has an R^2 value of 0.9951, the pseudo-second-order model has a better R^2 value. This demonstrates that the pseudo-second-order model is appropriate to represent the tetracycline on graphene oxide adsorption kinetics.

Table-1: Kinetics Parameters for the Adsorption of Tetracycline on Graphene Oxide

Adsorbent	Adsorbate	Kinetic Models			
		Pseudo-first-order		Pseudo-second-order	
		K1	R^2	K2	R^2
Graphene Oxide	Tetracycline	0.04021407614	0.8272	-0.5565	0.9951

The equilibrium results were further investigated using the Freundlich and Langmuir isotherm models, as Table-2 illustrates. Figure-8 and 9 illustrate the plots for the Langmuir and Freundlich isotherms, respectively. According to the correlation coefficient (R^2) value, both isotherm models may be used to predict how tetracycline would bind to graphene oxide, although the Langmuir model is preferable to the Freundlich model in this case. Table-2 contains the isotherm constants, which were computed using the slopes and intercepts of the linear plots. The Freundlich isotherm model constant (n) is connected to the adsorption capacity, whereas the constant of b is related to the adsorption energy of the Langmuir isotherm

model (L g^{-1}). The Langmuir isotherm model is predicated on the idea that adsorption is confined, restricted to monolayer coverage, and unrelated to the quantity of material adsorbed. In the Freundlich isotherm model, it is presumed that the heat of adsorption does not vary linearly with surface area but instead varies exponentially.[55]

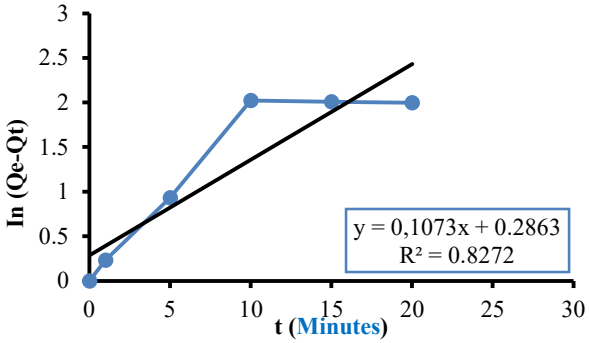

Fig.-5: Pseudo-First-Order Model

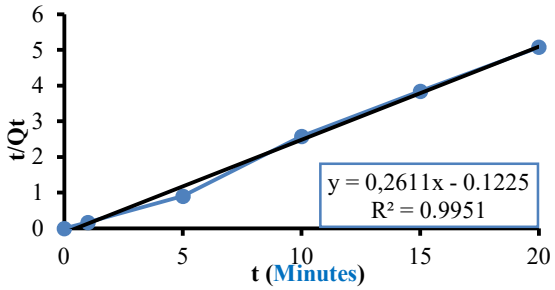

Fig.-6: Pseudo-Second-Order Model

Table-2: Parameters of Tetracycline Adsorption Isotherm on Graphene Oxide. (b is Langmuir Constant; n is Freundlich Constant)

Langmuir Model		Freundlich Model	
b	R^2	n	R^2
0.2958	0.9437	1.921968095	0.799

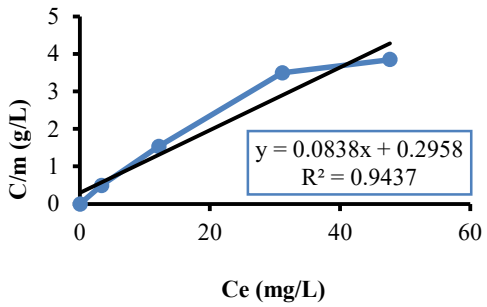

Fig.-8: The Linear Langmuir Isotherms Fitted to the Adsorption of Tetracycline

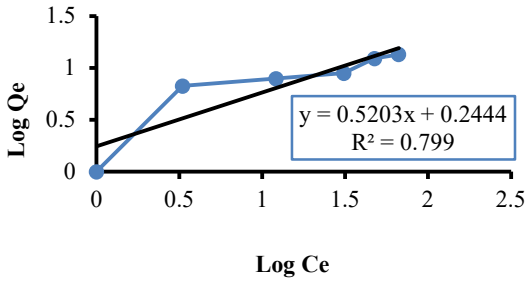

Fig.-7: The Linear Freundlich Isotherms Fitted to the Adsorption of Tetracycline

Adsorption Optimization

The following was researched and addressed on the impact of ideal conditions, including the mass of adsorbent, pH, initial adsorbate concentration, contact period, and desorption solvent.

Effect of Adsorbent Mass

Figure-10 depicts the impact of the adsorbent mass on the tetracycline adsorption by corn cob-derived graphene oxide. When the adsorbent mass was raised from 5 mg to 15 mg, the adsorption process increased noticeably from 32.79% to 59.02%. After the adsorbent mass of 15 mg, this adsorption level gradually rose. A mass of 20 mg of graphene oxide with a 62.26% adsorption rate produced the best results.

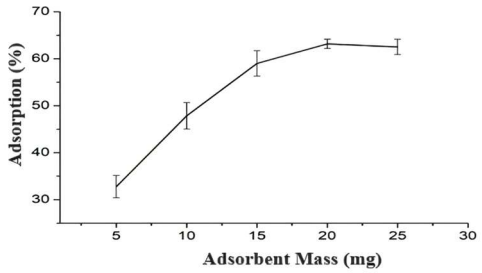

Fig.-8: Effect of the Adsorbent Mass on the Tetracycline Adsorption

The adsorption rate decreased when adsorbent masses of 25 mg were used; this is because the greater adsorbent mass results in density from overlap between adsorbent particles, which prevents the active side of the adsorbent from being maximized during the adsorbate absorption process.[56]

Effect of pH

Figure-11 illustrates how pH affects the graphene oxide's ability to bind tetracycline. At pH 5 (64.5%), the adsorbed state was at its best. The adsorption then significantly decreased at pH 5. Tetracyclines exist as cations at pH levels below 4 as a result of the dimethyl-ammonium group being protonated, according to Ghadim *et al.*[57] Tetracyclines occur as zwitterions at pH values of 3.5 to 7.5 as a result of the phenolic di-ketone group losing a proton. Due to the loss of a proton from the tri-carbonyl system and the di-ketone phenolic group, tetracycline exists as an anion at pH levels higher than 7. Additionally, according to Ali[58], graphene oxide's point of zero charge (PZC) generally ranges from 3.5 to 4. When the pH is less than or equal to the PZC, the surface charge of graphene oxide is positively charged; when the pH is more than or equal to the PZC, it is negatively charged. It was shown that graphene oxide experiences diverse degrees of deprotonation when subjected to different pH levels of adsorption. Because it has a positive charge at pH 3, graphene oxide repels cationic antibiotics via electrostatic attraction. At pH 5, on the other hand, the graphene oxide surface takes on a negative charge that improves the removal of cationic antibiotics. The graphene oxide goes through more deprotonation when the pH rises to 7.0, which raises its electronegativity. Tetracycline, on the other hand, doesn't charge up in neutral circumstances. As a result, in contrast to settings with acidic environments, the capacity of positively charged tetracycline to be adsorbed steadily declines. Since graphene oxide and tetracycline are both negatively charged at pH levels higher than 7, the electrostatic effect or electrostatic repulsion is greatly reduced. These results closely reflect those of research by Li *et al.*[40] that looked at how pH affected the adsorption of tetracycline antibiotics onto commercial graphene oxide.

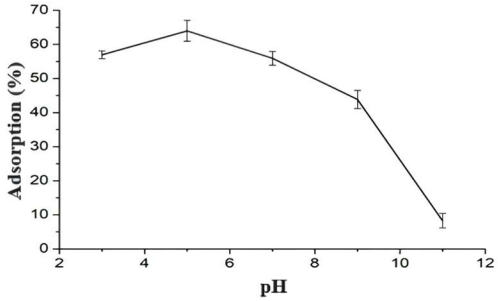

Fig.-9: Effect of pH on the Tetracycline Adsorption

Effect of Initial Adsorbate Concentration

Figure-12 illustrates how the starting concentration affected the tetracycline adsorption process. Adsorbate concentrations between 20 and 80 ppm were used, which reduced the adsorption rate. According to the results in Fig.-12, the tetracycline adsorption process by graphene oxide attained its ideal state at a concentration of 10 ppm with a 66.96% adsorption rate.

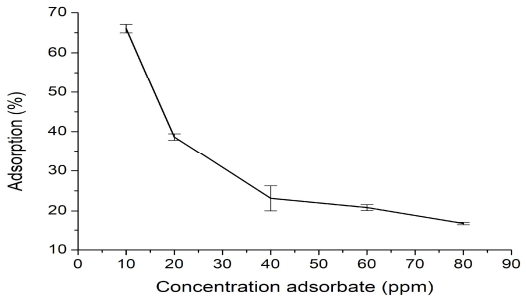

Fig.-10: Effect of the Initial Adsorbate Concentration on the Tetracycline Adsorption

As the adsorption capacity of the employed adsorbent decreases with falling adsorbate concentration, saturation occurs. Notably, at lesser concentrations, the adsorbate blocks the active sites, however, at larger concentrations, the blockage of the active sites in the structure of graphene oxide might rise and finally reach saturation. Up until equilibrium is reached, the amount of adsorbate bound to the adsorbent surface is greatly influenced by the length of contact between the graphene oxide adsorbent and the tetracycline solution. The adsorbent surface becomes saturated with the adsorbate after equilibrium has been reached. It is proposed that the adsorption capacity could increase with lower adsorbate concentrations. This behavior is comparable to the findings of the study done by Yadav *et al.*[59]

Effect of Contact Time

The outcomes depicted in Fig.-13 demonstrate a considerable improvement and a noticeable initial rise during the adsorption process. The adsorption process, however, showed a practically steady trend when the contact duration was increased over this cutoff, indicating that it had reached the equilibrium stage.

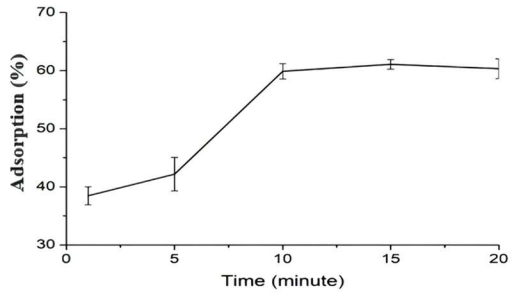

Fig.-11: Effect of the Contact Time on the Tetracycline Adsorption

This behavior highlights the complex interaction between tetracycline compounds and graphene oxide that controls the adsorption process. As the contact duration increases, the adsorbent becomes closer to saturation, which reduces the effectiveness of adsorption. Notably, this discovered trend matches the results of an experiment carried out concurrently by Chasanah *et al.*[60] The effectiveness of graphene oxide from cassava peel in removing tetracycline from the aquatic environment offers a basis for the development of more efficient water management systems, with the potential for integration into water treatment systems to reduce the impact of antibiotic residues on the environment and human health. However, the level of adsorption should be increased for a more effective reduction of antibiotic residues.

CONCLUSION

The findings of this study's tetracycline adsorption behavior on graphene oxide made from cassava peel are excellent. According to the results of its characterization, graphene oxide derived from cassava peel has

functional groups such as hydroxyl groups that allow for strong contact with its active sites. On the produced graphene oxide surface, tiny sheets of a smooth surface can be seen developing. According to kinetic studies, equilibrium is attained using the pseudo-second-order model in about 10 minutes. The Langmuir adsorption isotherm equations do a good job of describing the adsorption isotherms. An adsorbent mass of 20 mg, antibiotic concentration of 10 ppm, pH of 5, and contact time of 10 minutes are the ideal circumstances. As a potential adsorbent for the removal of tetracycline from aqueous environments, the promising material has showcased notable efficacy.

ACKNOWLEDGMENTS

The author expresses gratitude to the Ministry of Education, Cultural, Research and Technology, Republic of Indonesia's Directorate for Research, Technology and Community Services for providing research grants under the PDUPT research scheme, contract number 131/E5/PG.02.00.PL/2023 and 2624/UN26.21/PN/2023, as well as to other parties that have helped to directly or indirectly support the completion of this research.

CONFLICT OF INTERESTS

The authors declare that there is no conflict of interest.

AUTHOR CONTRIBUTIONS

All the authors contributed significantly to this manuscript, participated in reviewing/editing and approved the final draft for publication. The research profile of the authors can be verified from their ORCID ids, given below:

Rinawati http://orcid.org/0000-0002-4245-1729
P. Pirdaus https://orcid.org/0009-0006-4059-0721
A. Rahmawati https://orcid.org/0000-0003-2226-9521
Buhani https://orcid.org/0000-0003-2289-1804
A.A. Kiswandono https://orcid.org/0000-0002-8145-1959

REFERENCES

1. C. Yang, G. Song and W. Lim, *Comparative Biochemistry and Physiology Part C: Toxicology & Pharmacology,* **237**, 108840(2020), https://doi.org/10.1016/j.cbpc.2020.108840
2. Y. Ben, C. Fu, M. Hu, L. Liu, M.H. Wong and C. Zheng, *Environmental Research,* **169**, 483(2019), https://doi.org/10.1016/j.envres.2018.11.040
3. Y.Y. Chen, Y.L. Ma, J. Yang, L.Q. Wang, J.M. Lv and C.J. Ren, *Chemical Engineering Journal,* **307**, 15(2017), https://doi.org/10.1016/j.cej.2016.08.046
4. Sanjayadi and L.B. Violitas, *Galenika Journal of Pharmacy*, **6(2)**, 237(2020), https://doi.org/10.22487/j24428744.2020.v6.i2.15066
5. L. Xu, H. Zhang, P. Xiong, Q. Zhu, C. Liao and G. Jiang, *Science of the Total Environment,* **753**, 141975(2021), https://doi.org/10.1016/j.scitotenv.2020.141975
6. L. Serwecińska, *Water,* **12(12)**, 3313(2020), https://doi.org/10.3390/w12123313
7. A.L. Boroń, K. Kulik and K. Wyrzykowska, *Water,* **15(5)**, 975(2023), https://doi.org/10.3390/w15050975
8. S.A. Kraemer, A. Ramachandran and G.G. Perron, *Microorganisms,* **7(6)**, 180(2019), https://doi.org/10.3390%2Fmicroorganisms7060180
9. C.M. Loh, S. Mamphweli, E. Meyer and A. Okoh, *Molecules,* **23(4)**, 795(2018), https://doi.org/10.3390%2Fmolecules23040795
10. P. Grenni, V. Ancona and A.B. Caracciolo, *Microchemical Journal,* **136**, 25(2018), http://dx.doi.org/10.1016/j.microc.2017.02.006
11. L. Liu, W. Wu, J. Zhang and P. Lv, *Acta Rcologica Sinica,* **38(1)**, 36(2018),

http://dx.doi.org/10.1016/j.chnaes.2018.01.006
12. A. Rusu and E.L. Buta, *Pharmaceutics,* **13(12)**, 2085(2021), https://doi.org/10.3390%2Fpharmaceutics13122085
13. M. Cycoń, A. Mrozik and Z.P. Seget, *Frontiers in Microbiology,* **10**, 338(2019), https://doi.org/10.3389%2Ffmicb.2019.00338
14. A.H. Nguyen and S. Oh, *Journal of Hazardous Materials,* **455(4-5)**, 131571(2023), https://doi.org/10.1016/j.jhazmat.2023.131571
15. D.F. Calviño, M.C. Cid, A.N. Delgado, M.J.F. Sanjurjo, E.Á. Rodríguez and M.A. Estévez, *Processes,* **8(11)**, 1479(2020), https://doi.org/10.3390/pr8111479
16. M.S.D. Ilurdoz, J.J. Sadhwani and J.V. Reboso, *Journal of Water Process Engineering,* **45(5)**, 102474(2022), https://doi.org/10.1016/j.jwpe.2021.102474
17. M. Yan, A. Huang, J. Lin, L. Xu, H. Gong and H. Gong, *International Journal of Environmental Research and Public Health,* **18(9)**, 4909(2021), https://doi.org/10.3390%2Fijerph18094909
18. R. Guo, J. Chen, Q. Yang, Y. Gao, J. Ke, P.L. Show, Y. Ge and Y. Liu, *Bioengineered,* **12(1)**, 7376(2021), https://doi.org/10.1080%2F21655979.2021.1974657
19. M. Zahoor, M. Wahab, S.M. Salman, A.W. Kamran, S. Naz, J. Burlakovs, A. Kallistova, N. Pimenov and I. Zekker, *Water,* **13(14)**, 1969(2021), https://doi.org/10.3390/w13141969
20. N. Nasrollahi and V. Vatanpour, *The Science of the Total Environment,* **838(1)**, 156010 (2022), http://dx.doi.org/10.1016/j.scitotenv.2022.156010
21. G. Cravotto, E.C. Gaudino, E. Canova, P. Liu and Z. Wu, *Moleculs,* **26(3)**, 617(2021), https://doi.org/10.3390%2Fmolecules26030617
22. S. Zheng, Y. Wang, C. Chen, X. Zhou, Y. Liu, J. Yang, Q. Geng, G. Chen, Y. Ding and F. Yang, *International Journal of Environmental Research and Public Health,* **19(17)**, 10919(2022), https://doi.org/10.3390/ijerph191710919
23. F. Ahmad, D. Zhu and J. Sun, *Environmental Sciences Europe,* **33(64)**, 2021(2021), https://doi.org/10.1186/s12302-021-00505-y
24. B.O. Orimolade, A.O. Oladipo, A.O. Idris, F. Usisipho, S. Azizi, M. Maaza, S.L. Lebelo and B.B. Mamba, *Science of the Total Environment*, **881**, 163522(2023), https://doi.org/10.1016/j.scitotenv.2023.163522
25. L. Fu, D. Wu, H.K. Maleh and X. Liu, *Journal of Analytical Methods in Chemistry,* **2023,** 6443610(2023), https://doi.org/10.1155/2023/6443610
26. H.M.N. Iqbal, A.C. Cruz, A.R. Sanchez, G.G. Olivares, R.B.G. González, M.F.C. Alcaide and R.P. Saldívar, *Water Emerging Contaminants & Nanoplastics,* **2(2)**, 20517(2023), https://doi.org/10.20517/wecn.2022.19
27. A. Amari, F.M. Alzahrani, K.M. Katubi, N.S. Alsaiari, M.A. Tahoon and F.B. Rebah, *Materials,* **14(6)**, 1365(2021), https://doi.org/10.3390%2Fma14061365
28. R. Kayiwa, H. Kasedde, M. Lubwama and J.B. Kirabira, *Bioresource Technology Reports*, **15**, 100772(2021), https://doi.org/10.1016/j.biteb.2021.100772
29. D. Zhang, G. Crini, E. Lichtfouse, B. Rhimi and C. Wang, *Chemical Record, inPress,* **20(10)**, 1220(2020), https://doi.org/10.1002/tcr.202000073
30. S. Gueu, G. Finqueneisel, T. Zimny, D. Bartier and B.K. Yao, *Adsorption Science and Technology,* **37(1-2)**, 77(2018), http://dx.doi.org/10.1177/0263617418811469
31. N. Chen, M. Huang, C. Liu, G. Fang, G. Liu, Z. Sun, D. Zhou, J. Gao and C. Gu, *Water Research,* **165,** 114997(2019), https://doi.org/10.1016/j.watres.2019.114997
32. Darmadi, M.R. Lubis, M. Masrura, A. Syahfatra and Mahidin, *International Journal of Technology,* **14(1)**, 129(2023), https://doi.org/10.14716/ijtech.v14i1.5134
33. T. Altun, *Journal of the Chilean Chemical Society,* **65(2)**, 4790(2020), http://dx.doi.org/10.4067/S0717-97072020000204790
34. X. Liu, C. Wang, Q. Wu and Z. Wang, *Microchimica Acta,* **182**, 1903(2015), https://DOI:10.1007/s00604-015-1530-8
35. Buhani, S.N. Halimah, Suharso and Sumadi, *Rasayan Journal Chemistry,* **15(1)**, 124(2022), http://dx.doi.org/10.31788/RJC.2022.1516538

36. R. Rakkimuthu, S. Aarthi, E. Neelamathi, P. Sathishkumar, A.M. Anandakumar and D. Sowmiya, *Rasayan Journal Chemistry,* **15(1)**, 417(2022), http://dx.doi.org/10.31788/RJC.2022.1516786
37. H. Chen, B. Gao and H. Li, *Journal of Hazardous Materials*, **282**, 201(2015), http://dx.doi.org/10.1016/j.jhazmat.2014.03.063
38. C. Rodríguez, C. Tapia, E.L. Aravena and E. Leiva, *International Journal of Environmental Research and Public Health,* **17(18)**, 6911(2020), https://doi.org/10.3390/ijerph17186911
39. K. Thakur and B. Kandasubramanian, *Journal of Chemical and Engineering Data,* **64(3)**, 833(2019), https://doi.org/10.1021/acs.jced.8b01057
40. Z. Li, H. Jiang, X. Wang, C. Wang and X. Wei, *International Journal of Environmental Research and Public Health,* **20(3)**, 2448(2023), https://doi.org/10.3390/ijerph20032448
41. B. Silva, M. Martins, M. Rosca and V. Rocha, *Separation and Purification Technology*, **235,** 116139(2020), http://dx.doi.org/10.1016/j.seppur.2019.116139
42. Bureau of Central Statistics, *Cassava Plants Per-Province in Indonesia,* (2018), https://www.bps.go.id/id/publication/2018/07/03/5a963c1ea9b0fed6497d0845/statistik-indonesia-2018.html
43. L. Sun, *Chinese Journal of Chemical Engineering*, **27(10)**, 2251(2019), https://doi.org/10.1016/j.cjche.2019.05.003
44. F. Li, D.L. Zhao, L.Z. Bai and D.D. Zhang, *Applied Mechanics and Materials,* **320**, 540(2013), http://dx.doi.org/10.4028/www.scientific.net/AMM.320.540
45. A. Schedy, D. Quarthal and M. Oetken, *World Journal of Chemical Education,* **6(1)**, 43(2018), https://DOI:10.12691/wjce-6-1-8
46. G.K. Dongo, N.J. Nsami and K.J. Mbadcam, *BioResources,* **15(2)**, 2133(2020), https://doi.org/10.15376/biores.15.2.2133-2146
47. E.H. Sujiono, Zurnansyah, D. Zabrian, M.Y. Dahlan, B.D. Amin, Samnur and J. Agus, *Heliyon,* **6(8)**, 4568(2020), https://doi.org/10.1016/j.heliyon.2020.e04568
48. B. Yu, Y. Bai, Z. Ming, H. Yang, L. Chen, X. Hu, S. Feng and T.S. Yang, *Materials Chemistry and Physics*, **198**, 283(2017), https://doi.org/10.1016/j.matchemphys.2017.05.042
49. H.A.S. Tohamy, M. El-Sakhawy and S. Kamel, *Journal of Polymer Research*, **29(75)**, 21(2022), https://doi.org/10.1007/s10965-021-02830-5
50. T. Somanathan, K. Prasad, K.K. Ostrikov, A. Saravanan and V.M. Krishna, *Nanomaterials*, **5(2)**, 826(2015), https://doi.org/10.3390/nano5020826
51. Y. Ai, Y. Liu, Y. Huo, C. Zhao, L. Sun, B. Han, X. Cao and X. Wang, *Environmental Science Nano*, **6(11)**, 3336(2019), https://doi.org/10.1039/C9EN00866G
52. C. Yu, C.F. Wang and S. Chen, *Scientific Reports,* **6**, 17071(2016), https://doi.org/10.1038/srep17071
53. Y. Zhuang, F. Yu, J. Ma and J. Chen, *New Journal of Chemistry,* **5(39)**, 3333(2015), https://doi.org/10.1039/c5nj00019j
54. Y. Lin, S. Xu and L. Jia, *Chemical Engineering Journal*, **225**, 679(2013), http://dx.doi.org/10.1016/j.cej.2013.03.104
55. E.Ç. Salihi, J. Wang, G. Kabacaoğlu, S. Kırkulak and L. Šiller, *Separation Science and Technology,* **56(3)**, 453(2020), https://doi.org/10.1080/01496395.2020.1717533
56. N.K. Mondal, R. Bhaumik, A. Banerjee, J.K. Datta and T. Baur, *International Journal of Environmental Sciences,* **2(3)**, 1643(2012), https://doi.org/10.6088/IJES.00202030049
57. E.E. Ghadim, F. Manouchehri, G. Soleimani, H. Hosseini, S. Kimiagar and S. Nafisi, *Plos One,* **8(11)**, 79254(2013), https://doi.org/10.1371/journal.pone.0079254
58. J. Ali, Y. Li, E. Shang, X. Wang, J. Zhao, M. Mohiuddin and X. Xia, *Chinese Chemical Letters,* **34(2)**, 107327(2023), https://doi.org/10.1016/j.cclet.2022.03.050
59. A. Yadav, R. Kumar, H.K. Choudhary and B. Sahoo, *Carbon,* **140(84)**, 477(2018), https://doi.org/10.1016/j.carbon.2018.08.062
60. U. Chasanah, W. Trisunaryanti, Triyono, H.S. Oktaviano and D.A. Fatmawati, *Rasayan Journal Chemistry,* **14(3)**, 2017(2021), http://doi.org/10.31788/RJC.2021.1436042

[RJC- 8640/2023]